World Academy of Science, Engineering and Technology
International Journal of Biomedical and Biological Engineering
Vol:15, No:12, 2021

Development of Electrospun Membranes with Defined Polyethylene Collagen and Oxide Architectures Reinforced with Medium and High Intensity Statins

S. Jaramillo, Y. Montoya, W. Agudelo, J. Bustamante

***Abstract*—**Cardiovascular diseases (CVD) are related to affectations of the heart and blood vessels, within these are pathologies such as coronary or peripheral heart disease, caused by the narrowing of the vessel wall (atherosclerosis), which is related to the accumulation of Low-Density Lipoproteins (LDL) in the arterial walls that leads to a progressive reduction of the lumen of the vessel and alterations in blood perfusion. Currently, the main therapeutic strategy for this type of alteration is drug treatment with statins, which inhibit the enzyme 3-hydroxy-3-methyl-glutaryl-CoA reductase (HMG-CoA reductase), responsible for modulating the rate of cholesterol production and other isoprenoids in the mevalonate pathway. This enzyme induces the expression of LDL receptors in the liver, increasing their number on the surface of liver cells, reducing the plasma concentration of cholesterol. On the other hand, when the blood vessel presents stenosis, a surgical procedure with vascular implants is indicated, which are used to restore circulation in the arterial or venous bed. Among the materials used for the development of vascular implants are Dacron® and Teflon®, which perform the function of re-waterproofing the circulatory circuit, but due to their low biocompatibility, they do not have the ability to promote remodeling and tissue regeneration processes. Based on this, the present research proposes the development of a hydrolyzed collagen and polyethylene oxide electrospun membrane reinforced with medium and high-intensity statins, so that in future research it can favor tissue remodeling processes from its microarchitecture.

***Keywords*—**Atherosclerosis, medium and high-intensity statins, microarchitecture, electrospun membrane.

I. Introduction

CARDIOVASCULAR disease (CVD) is a group of heart and blood vessel disorders including heart failure, arrhythmias, hypertension, cerebrovascular accidents, congenital heart disease, peripheral vascular disease, and coronary artery (CC) disease [1]. These last two diseases have the highest incidence due to the narrowing of the lumen of the blood vessels due to the stiffness or thickening of the vascular wall (arteriosclerosis) and the accumulation of LDL (atherosclerosis) [2]-[5]. Under this scenario, atherosclerosis generates processes of stenosis and decreased hemodynamic perfusion causing occlusion of the blood vessel, which leads to impairments in the functionality of tissues and organs [6]-[8]. To minimize the effect of this type of pathology, pharmacological treatments with statins [9], [10] are used, which modulate the production rate of cholesterol and isoprenoids, as well as the absorption and catabolism of plasma LDL, leading to the reduction of cardiovascular events; because they can reduce the level of LDL cholesterol by 1.8 mmol/L (70 mg/dL) [9], [11], [12].

Another treatment for vascular stenosis is the surgical procedure through the use of vascular grafts, which partially or totally restore circulation in the arterial or venous bed, emulating the dynamic behavior of a native vessel. Currently, the materials used to re-establish circulation in the arterial bed as medical devices are Dacron® and Teflon®, which have exhibited similar characteristics to native vessels, but it has been shown that after implantation there are alterations in hemodynamic variables of the proximal regions by decreasing coronary perfusion and increasing ventricular afterload, added to the low capacity to promote tissue remodeling and regeneration processes [2], [13]-[16].

Due to the problems presented by synthetic vascular implants that lead to a decrease in the coronary artery bed, added to the stress on the surrounding tissue and the low rate of degradation, the use of materials of natural origin over synthetic materials is proposed for the development of bioactive implants, due to the ability to biointegrate with native tissue in short periods of time, minimizing the risks of thrombosis and favoring tissue remodeling processes [17]-[23].

Among the materials of natural origin, the use of collagen for the development of three-dimensional structures favors the processes of cell adhesion and minimizes the number of platelets deposited on the wall of the biomaterial that can lead to the formation of thrombi. The above added to the ability of collagen to generate fibrillar structures through physical transformation techniques that emulate the microarchitecture of the native extracellular matrix of the vessels, which give rise to porous surfaces that promote the formation of the endothelium. The latter being of primary importance due to these implants must present controllable pore sizes and porosities that favor

Santiago Jaramillo, Wilson Agudelo and John Bustamante are with the Grupo de Dinámica Cardiovascular, Centro de Bioingeniería, Universidad Pontificia Bolivariana, Colombia (phone: +57(4) 448 8388 ext: 12400, e-mails: santiago.jaramillor@upb.edu.co, wilson.agudelo@upb.edu.co, john.bustamante@upb.edu.co).

Yuliet Montoya is with the Grupo de Dinámica Cardiovascular, Centro de Bioingeniería Universidad Pontificia Bolivariana, Colombia (corresponding author, e-mail: yuliet.montoya@upb.edu.co).

cell permeabilization and minimize blood loss [24]-[26].

Based on this, the present research evaluated the influence of the incorporation of medium and high-intensity statins on the microarchitecture of hydrolyzed collagen and polyethylene oxide electrospun membranes for the development of a bioactive material that could be an alternative therapeutic strategy to the use of synthetic vascular grafts and reduce the recurrence of angioplasty surgical processes caused by high concentrations of LDL.

II. Materials and Methods

A. Materials

For this investigation, hydrolyzed collagen (Col-H) and polyethylene oxide (PEO) were obtained from Sigma Aldrich. Atorvastatin (Atv) of 20 and 40 mg were obtained from commercial tablets. Methanol (CH_3OH) was obtained from Merck Millipore.

B. Preparation of Col-H and PEO Solutions

For the control samples, Col-H solutions were prepared at concentrations of 7 % w/v and PEO at concentrations of 4 and 5 % w/v using deionized water as solvent. Then, mixtures were made at volumetric ratios of PEO: Col-H from 50:50 to 70:30 %, which were homogenized by 30 min.

C. Preparation of Solutions of Col-H and PEO Functionalized with Medium and High Intensity Atorvastatin

For the experimental design of electrospun membranes with medium and high intensity statin, 20 and 40 mg of atorvastatin were diluted in pure methanol. Optimal points of the mixture without atorvastatin were taken into account and the volumetric ratios will be varied between 3 and 20% of the active principle of the drug.

D. Electrospinning

The control and statin-fortified solutions were loaded into a 5 mL glass syringe and electrospun at fixed voltage conditions of 19 kV, flow of 0.7 mL/h, varying the needle-collector distance between 15 - 25 cm and the rotation speed of collector between 50 and 250 rpm.

E. Scanning Electron Microscopy (SEM) Analysis

The morphological characteristics of the surface and fiber size of the membranes were analyzed in a Jeol NeoScope JCM-6000 Plus scanning electron microscope operated at 15 kV. For SEM evaluation, samples of each membrane were fixed on metallic supports with a conductive graphite tape and a thin coating with gold was carried out to provide a contact of the material with the loading beam. The analysis was carried out at magnifications of 2000, 5000 and 10000*X*.

F. Fourier-Transform Infrared Spectroscopy Analysis

The IR spectra of the electrospun scaffolds without and with medium and high-intensity atorvastatin were obtained at wavelengths between 4000 - 400 cm^{-1} using a Nicolet iS50 FTIR spectrometer with attenuated total reflectance (ATR) module at a resolution of 4 cm^{-1} and 64 scans.

G. Statistical Analysis

For the statistical analysis of the fiber diameter of the SEM images, the ImageJ® software was used, then the data were processed in the Statgraphics Centurion XVI software, which allowed obtaining the population mean, the standard deviation and the confidence intervals of the 95%.

III. Results and Discussion

A. Evaluation of the Microarchitecture of PEO: Col-H Electrospun Membranes with and without the Incorporation of Statins

To develop PEO:Col-H electrospun membranes reinforced and not reinforced with medium and low-intensity statins with continuous fibers and without alterations in their morphology, different experimental designs were proposed varying the electrospinning conditions (see Table I), of which it was found that the SEM micrographs showed that as the natural polymer ratio increased, pearl and aggregate-like defects appeared on the fibers, as observed in the membranes obtained at PEO: Col-H ratios of 50:50, 60:40, and 70:30 (see Fig. 1). The above is attributed to the increase in the proportion of Col-H in the solution, which led to changes in the apparent viscosities of the solutions as a result of a greater presence of the solvent used for the mixture, which did not evaporate during the fly time of the fiber until the deposition in the rotational collector [27], [28]. On the other hand, it was observed that by increasing the collection distance for the membranes obtained at PEO:Col-H ratios of 50:50 (see Figs. 1 (A)-(C)), there was a decrease in the number of defects present in the fibers, as well as in the volume of sample collected compared to the membranes obtained at ratios of 60:40 (see Figs. 1 (D)-(F)) and 70:30 (see Figs. 1 (G)-(I)), where a decrease in defects and low variability in the volume of fibers collected. This can be attributed to the increase in the volumetric ratio of PEO, which supported the solution by increasing the apparent viscosity [29]. On the other hand, by increasing the collection distance to 25 cm for the membranes at volumetric ratios of 60:40 (see Fig. 1 (F)) and 70:30 (see Fig. 1 (I)), a greater discontinuity was evidenced in the fibers in comparison to those obtained at a distance of 20 cm. That behavior could be attributed to the evaporation of the solvent present in the electrospun material that prevented the polymer chains of the PEO:Col-H mixture from elongating before being deposited in the collector.

TABLE I
Initial Conditions for Electrospun of PEO:Col-H Membranes

Parameter	Unit	Value
Flow	mL/h	0.7
Voltage	KV	19
Wetness	%	20 - 30
Distance	cm	15 – 20 – 25
Volumetric Relations PEO:Col—H	%	50:50, 60:40, 70:30
Rotation speed	rpm	250

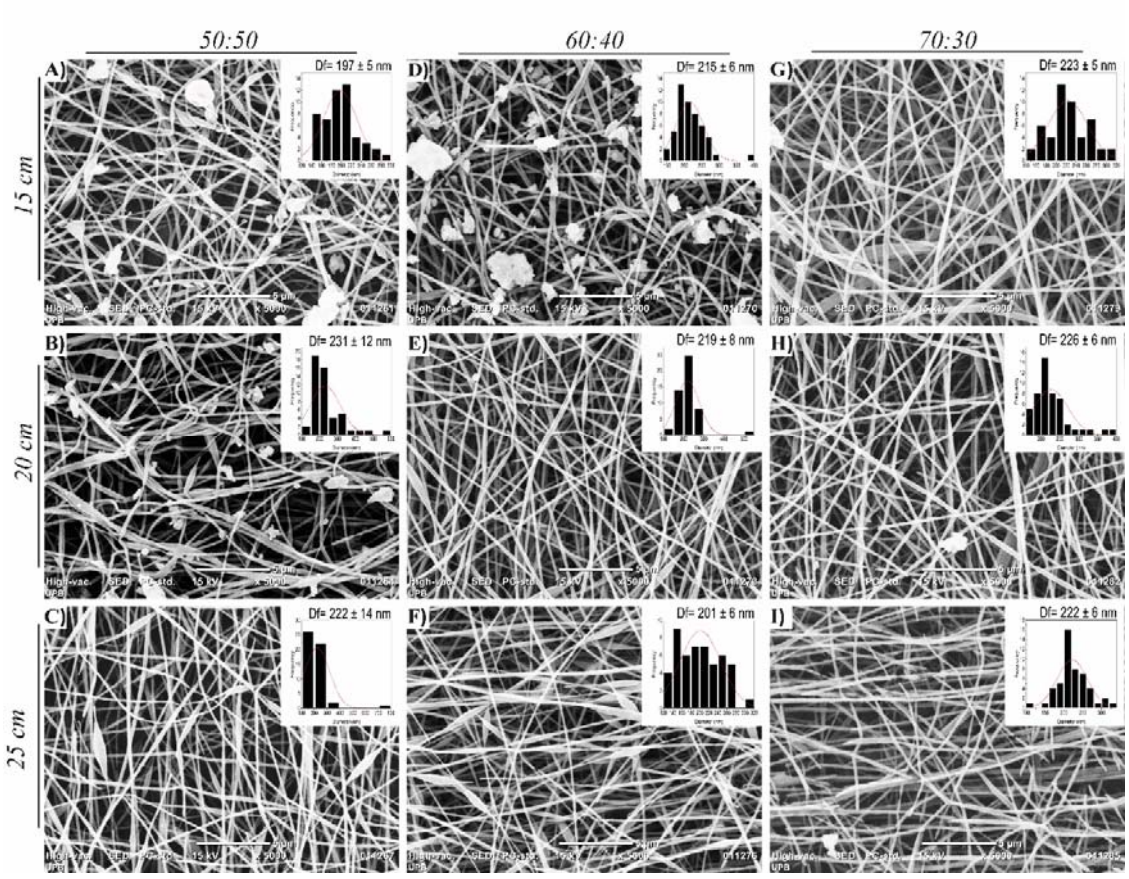

Fig. 1 SEM micrographs of Col-H: PEO electrospun membranes at 250 rpm, obtained at a volumetric ratio of 50:50 and a distance of (A) 15 cm, (B) 20 cm, and (C) 25 cm; at a volumetric ratio of 40:60 and distance from (D) 15 cm, (E) 20 cm, and (F) 25 cm; and at a volumetric ratio of 30:70 and distance from (G) 15 cm, (H) 20 cm, and (I) 25 cm. 5 μm scale bar

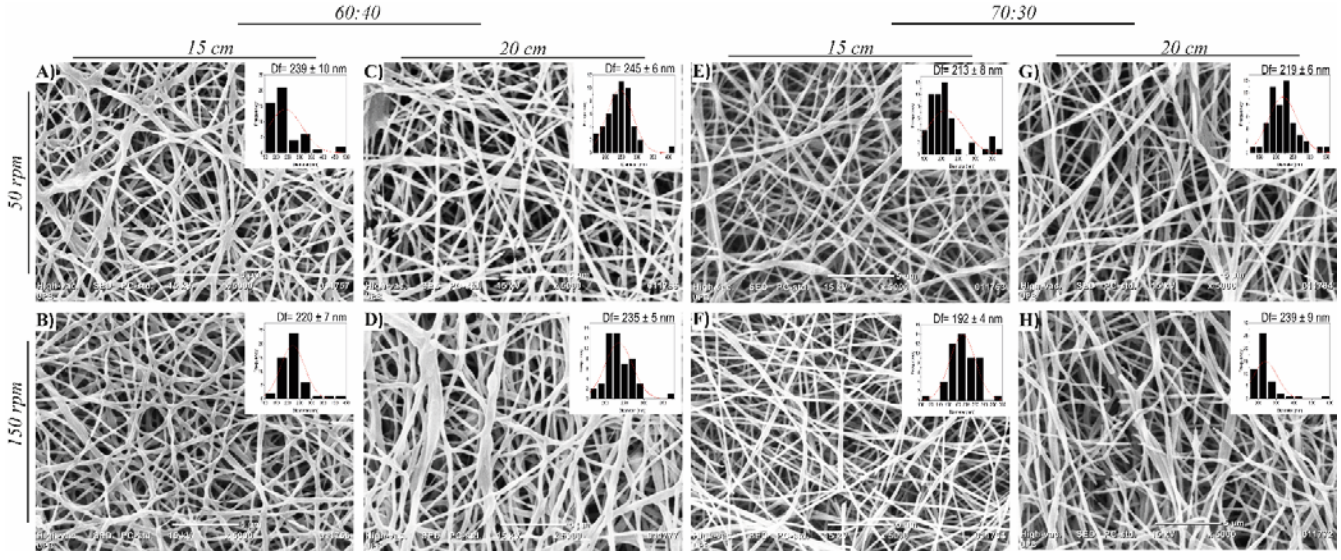

Fig. 2 SEM micrographs of electrospun PEO: Col-H membranes obtained at a volumetric ratio of 60:40 (A) 15 cm and 50 rpm, (B) 15 cm and 150 rpm; (C) 20 cm and 50 rpm, (D) 20 cm and 150 rpm. At a volumetric ratio of 70:40 (E) 15 cm and 50 rpm, (F) 15 cm and 150 rpm; (G) 20 cm and 50 rpm, (H) 20 cm and 150 rpm. 5 μm scale bar

In addition to the foregoing, changes were made in the electrospinning conditions (see Table II), finding that as the distance/speed relationship increased, an increase in the number of discontinuous fibers present in the membranes obtained at ratio of PEO:Col-H of 60:40 (see Figs. 2 (A)–(D)) and 70:30 (see Figs. 2 (E)-(H)). This is associated with a fast evaporation

of the solvent before deposition in the collector and the stretching of the fibers at higher rotation speeds. On the other hand, by increasing the Col-H volumetric ratios in the polymer mixture, there are significant differences in the final microarchitecture of the membranes, due to the fact that the interconnectivity of the fibers and the presence of pearl-shaped defects are not favored [30].

TABLE II
INTERMEDIATE CONDITIONS FOR ELECTROSPUN OF PEO:COL-H MEMBRANES

Parameter	Unit	Value
Flow	mL/h	0.7
Voltage	KV	19
Wetness	%	20 - 30
Distance	cm	15 – 20
Volumetric Relations PEO:Col—H	%	60:40, 70:30
Rotation speed	rpm	50-150

Taking into account that the effect of the distance/speed relationship on the microarchitectures of PEO:Col-H membranes, the conditions of collection distance and rotation speed were modified (see Table III), finding from the analysis of the SEM micrographs fiber diameters of 240 ± 4 nm and 250 ± 4 nm for the membranes obtained at distances of 15 cm and volumetric ratios of 60:40 (see Fig. 3 (A)) and 70:30 (see Fig. 3 (C)), respectively. On the other hand, for the membranes obtained at a distance of 20 cm, the presence of discontinuous fibers with diameters of 289 ± 11 nm for the 60:40 ratio (see Fig. 3 (B)) and 279 ± 3 nm for the 70:30 ratio was evidenced (see Fig. 3 (D)). From the above, it is evident that changes in the distance/speed relationship not only lead to an increase in the number of fibers with discontinuity but also increase the fiber diameter as a result of a voltage/distance relationship (kV/cm) that leads to the fiber of the polymers that make up the PEO:Col-H mixture are not elongated or that prevent the total evaporation of the solvent [31].

TABLE III
FINAL CONDITIONS FOR ELECTROSPUN OF PEO:COL-H MEMBRANES

Parameter	Unit	Value
Flow	mL/h	0.7
Voltage	KV	19
Wetness	%	20 - 30
Distance	cm	15 – 20
Volumetric Relations PEO:Col—H	%	60:40, 70:30
Rotation speed	rpm	250

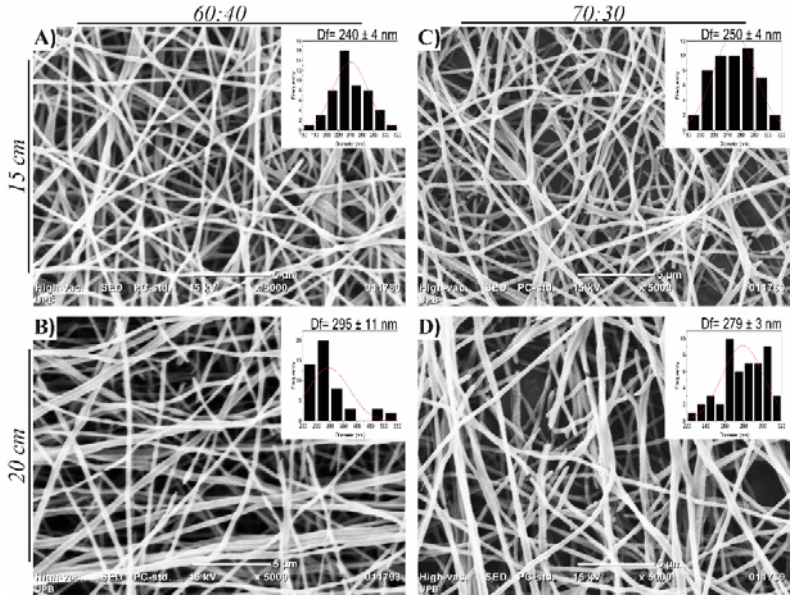

Fig. 3 SEM micrographs for electrospun PEO-Col-H membranes at a ratio of 60:40 (A) 15 cm, (B) 20 cm. At a ratio of 70:30 (C) 15 cm, (D) 20 cm. 5 μm scale bar

Finally, to obtain electrospun PEO:Col-H membranes with continuous and uniform fibers, without the presence of pearl-type defects, with diameters between 190-250 nm and which in turn can favor ideal environments for migration, adhesion and proliferation of smooth muscle and endothelial cells (SMC), the electrospinning conditions of volumetric ratio PEO:Col-H of 60:40, collector speed of 250 rpm and needle-collector distance of 15 cm were established, which they were used for the incorporation of medium and high-intensity statins.

Based on the foregoing, it was evaluated how the incorporation of different concentrations of atorvastatin in the electrospinning process modified the microarchitecture of the PEO:Col-H membranes. For this, solutions prepared at volumetric ratios of PEO:Col-H/Atv of 97/3, 95/5, 90/10, 85/15, and 80/20 were electrospun, finding from SEM micrographs (see Fig. 4), that the incorporation of medium and high intensity Atv in the electrospinning process does not lead to the obtaining of pearl-shaped defects in the membranes. On the other hand, as the Atv ratio increased, the fiber diameter decreased obtaining fiber diameters of 212 ± 4 nm and 198 ± 3 nm for the membranes obtained at a ratio of 80/20 with Atv of 20 mg (see Fig. 4 (E)) and 40 mg (see Fig. 4 (J)) respectively,

compared to the diameters of 218 ± 3 nm and 201 ± 4 nm obtained at a 95:5 ratio with Atv of 20 mg (see Fig. 4 (B)) and 40 mg (see Fig. 4 (G)). On the other hand, it was determined that the 80:20 and 95:5 ratios lacked pearl-like defects and the fibers exhibited a unidirectional tendency on the part of the fibers.

Taking into account that it is sought to have a higher concentration of atorvastatin incorporated in the fibers, without alterations such as beads or aggregates, continuity and optimal fiber collection, in addition to appropriate morphology for the migration and proliferation of SMC, it is decided to continue future research with volumetric relation of PEO:Col-H/Atv of 80:20 ratio.

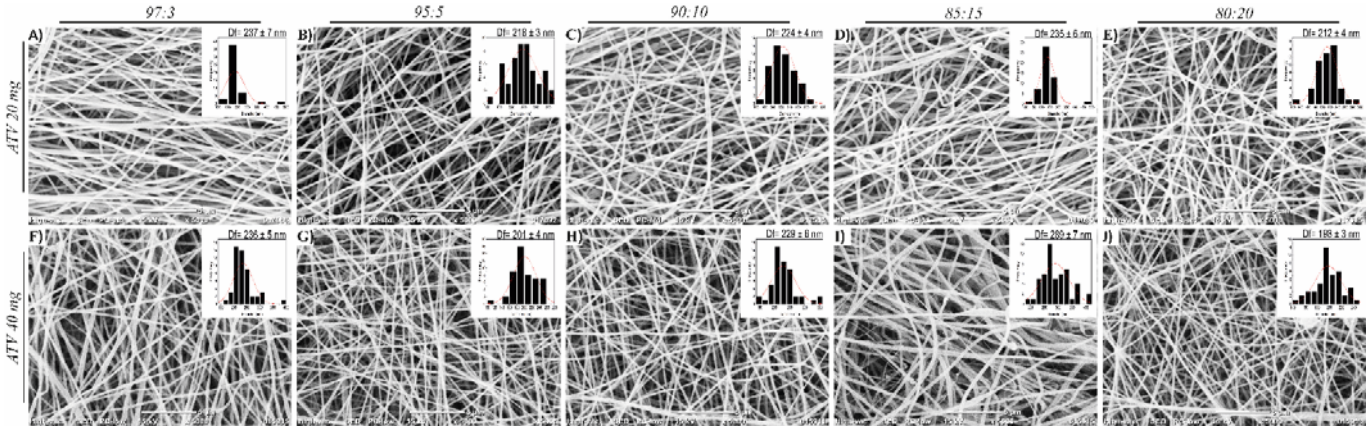

Fig. 4 SEM micrographs of PEO:Col-H reinforced with 20 mg of atorvastatine with relation of PEO:Col-H/Atv of (A) 97:3, (B) 95:5, (C) 90:10, (D) 85/15, and (E) 80/20. With 40 mg of atorvastatine with relation of PEO:Col-H/Atv of (F) 97:3, G) 95:5, (H) 90:10, (I) 85/15, and (J) 80/20. 5 μm scale bar

B. Evaluation of the Incorporation of Atorvastatin in the Electrospun Membranes of PEO Col-H/Atv

To evaluate the changes in the functional groups of the electrospun PEO:Col-H membranes without and with the incorporation of medium and high-intensity atorvastatin, the analysis by infrared spectroscopy was performed, finding that for the case of the PEO:Col-H (see Fig. 5 (A)) the presence of an absorption band at 3291 cm^{-1} associated with the N-H stretching of amide A was evidenced, which could be related to the formation of hydrogen bonds that contribute to conservation triple helix of the protein, establishing that electrospinning processes do not lead to structural modifications of Col-H [32]. Likewise, the presence of absorption bands was observed at 2947 cm^{-1} associated with the asymmetric stretching of CH_2 of amide B, 1633 cm^{-1} of amide I, 1540 cm^{-1} amide II, and at 1234 cm^{-1} for amide III [33]. Concerning PEO, characteristic bands were found at 2882 cm^{-1} related to the stretching of the CH_2 group, 1094 cm^{-1} corresponding to the stretching of C-O-C and at 962 cm^{-1} of C-H [34]. For the case of membranes with Atv at different relationships (see Fig. 5 (B)), bands were evidenced at 3358 cm^{-1} related to stretching of the OH group, 2916 cm^{-1} attributed to the presence of CH_2, at 1659 and 1422 cm^{-1} corresponding to the C=O stretch of carboxylic acid and amide N-H, respectively, and 1057 cm^{-1} of the C-N group stretch [35]. Likewise, when performing the analysis for samples of atorvastatin 40 mg under the same conditions as Atv 20 mg (Fig. 6), these presented characteristic peaks of atorvastatin, including a C=O double bond in the 1641 cm^{-1}, double bond C=O of an amide 1435 cm^{-1}, O-H group stretching 3348 cm^{-1} and CN stretching 1042 cm^{-1} [36].

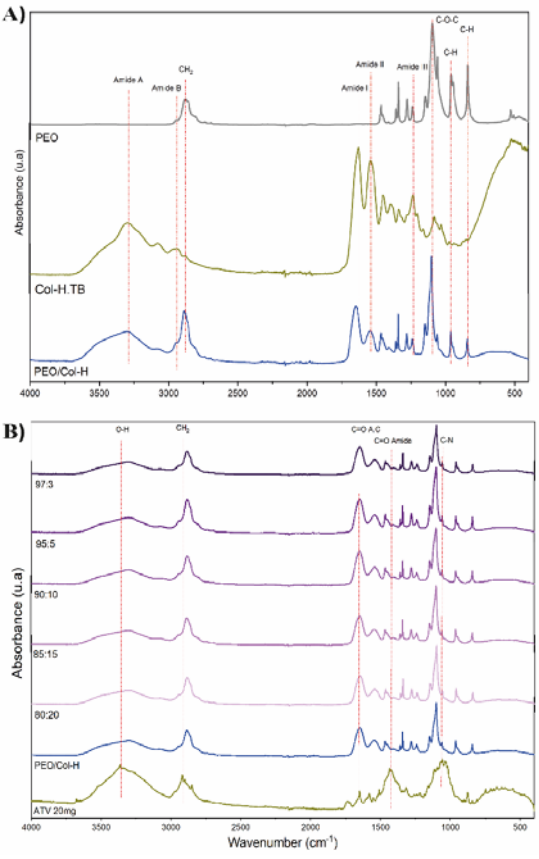

Fig. 5 IR absorption spectra for (A) PEO:Col-H electrospun membranes; (B) PEO_Col-H/Atv 20 mg electrospun membranes: at different volumetric ratios. Thin films were used for the PEO and Col-H controls

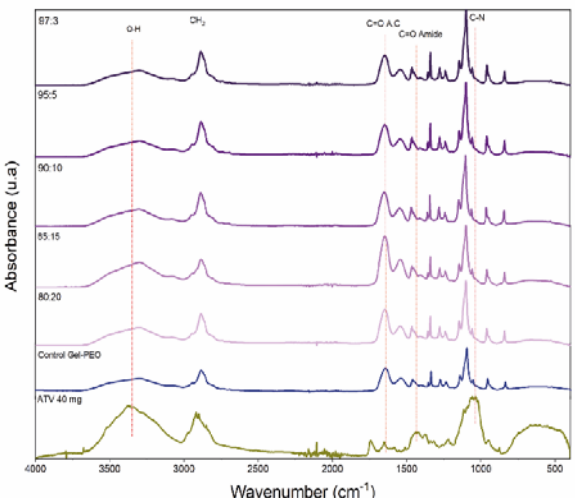

Fig. 6 IR absorption spectra PEO:Col-H/Atv 40 mg electrospun membranes: at different volumetric ratios

IV. Conclusion

An electrospun PEO: Col-H/Atv membrane was obtained composed of nanometric fibers that present a fibrillar microarchitecture without the presence of defects and a rearrangement of the fibers compared to electrospun membranes only PEO: Col-H, which indicates that these types of materials are a good candidate for the development of bioactive vascular implants. On the other hand, the FTIR-ATR analyzes show the presence of atorvastatin in the fibrillar microarchitecture of electrospun membranes. Which indicates that Atv is the modulator compound of the fibrillar structure of the material and that in future research these membranes could be used to avoid the narrowing and decrease of hemodynamic perfusion in blood vessels as a result of vascular conditions such as atherosclerosis that compromise the functioning of tissues and organs, in addition to promoting SMC proliferation and migration.

Acknowledgment

The authors thank the Universidad Pontificia Bolivariana for the academic support in the formation of a student resource committed in the present research work. Also, to the Ministry of Science, Technology and Innovation - MINCIENCIAS, Colombia, for the academic support in the formation of a student resource in the announcement of national doctorate 647 of 2014, call Young Researchers and Innovators 812-2018 and project 121084467592 MINCIENCIAS.

References

[1] G. A. Roth *et al.*, "Global Burden of Cardiovascular Diseases and Risk Factors, 1990–2019: Update from the GBD 2019 Study," *Journal of the American College of Cardiology*, vol. 76, no. 25. Elsevier Inc., pp. 2982–3021, 22-Dec-2020.

[2] H. A. Strobel, E. I. Qendro, E. Alsberg, and M. W. Rolle, "Targeted delivery of bioactive molecules for vascular intervention and tissue engineering," *Front. Pharmacol.*, vol. 9, no. November, pp. 1–23, 2018.

[3] Y. M. Ju, J. S. Choi, A. Atala, J. J. Yoo, and S. J. Lee, "Bilayered scaffold for engineering cellularized blood vessels," *Biomaterials*, vol. 31, no. 15, pp. 4313–4321, 2010.

[4] Z. Tan, H. Wang, X. Gao, T. Liu, and Y. Tan, "Composite vascular grafts with high cell infiltration by co-electrospinning," *Mater. Sci. Eng. C*, vol. 67, pp. 369–377, 2016.

[5] W. Zeng, Y. Li, Y. Wang, and Y. Cao, "Tissue engineering of blood vessels," in *Encyclopedia of Tissue Engineering and Regenerative Medicine*, vol. 1–3, Elsevier Inc., 2019, pp. 413–424.

[6] M. Kuk, N. C. Ward, and G. Dwivedi, "Extrinsic and Intrinsic Responses in the Development and Progression of Atherosclerosis," *Heart Lung and Circulation*. Elsevier Ltd, 16-Jan-2021.

[7] S. Barquera *et al.*, "Global Overview of the Epidemiology of Atherosclerotic Cardiovascular Disease," *Arch. Med. Res.*, vol. 46, no. 5, pp. 328–338, Jul. 2015.

[8] R. Pahwa and I. Jialal, "Atherosclerosis," *Diet, Exerc. Chronic Dis. Biol. Basis Prev.*, pp. 133–210, Aug. 2020.

[9] I. Pinal-Fernandez, M. Casal-Dominguez, and A. L. Mammen, "Statins: pros and cons," *Medicina Clinica*, vol. 150, no. 10. Ediciones Doyma, S. L., pp. 398–402, 23-May-2018.

[10] S. Mennickent C, M. Bravo D., C. Calvo M, and M. Avello L, "Efectos pleiotrópicos de las estatinas," *Rev. Med. Chil.*, vol. 136, no. 6, pp. 775–782, Jun. 2008.

[11] B. Mihaylova *et al.*, "The effects of lowering LDL cholesterol with statin therapy in people at low risk of vascular disease: Meta-analysis of individual data from 27 randomised trials," *Lancet*, vol. 380, no. 9841, pp. 581–590, Aug. 2012.

[12] E. Biros, J. E. Reznik, and C. S. Moran, "Role of inflammatory cytokines in genesis and treatment of atherosclerosis," *Trends Cardiovasc. Med.*, Feb. 2021.

[13] Q. Langouet *et al.*, "Incidence, predictors, impact, and treatment of vascular complications after transcatheter aortic valve implantation in a modern prospective cohort under real conditions," *J. Vasc. Surg.*, vol. 72, no. 6, pp. 2120-2129.e2, Dec. 2020.

[14] Q. Zhang *et al.*, "Heparinization and hybridization of electrospun tubular graft for improved endothelialization and anticoagulation," *Mater. Sci. Eng. C*, vol. 122, no. January, p. 111861, 2021.

[15] I. Cicha, R. Singh, C. Garlichs, and C. Alexiou, "Nano-biomaterials for cardiovascular applications: Clinical perspective," *J. Control. Release*, vol. 229, pp. 23–36, 2016.

[16] A. Subramaniam and S. Sethuraman, "Biomedical Applications of Nondegradable Polymers," in *Natural and Synthetic Biomedical Polymers*, Elsevier Inc., 2014, pp. 301–308.

[17] Y. M. Ju *et al.*, "Electrospun vascular scaffold for cellularized small diameter blood vessels: A preclinical large animal study," *Acta Biomater.*, vol. 59, pp. 58–67, 2017.

[18] D. M. García Cruz, "Materiales macroporosos biodegradables basados en quitosano para la ingeniería tisular," pp. 1–223, 2008.

[19] S. N. Hanumantharao and S. Rao, "Multi-functional electrospun nanofibers from polymer blends for scaffold tissue engineering," *Fibers*, vol. 7, no. 7, pp. 1–35, 2019.

[20] D. A. Florea, V. Grumezescu, A. M. Grumezescu, and E. Andronescu, "Clinical applications of bioactive materials," in *Materials for Biomedical Engineering: Bioactive Materials, Properties, and Applications*, V. Grumezescu and A. M. Grumezescu, Eds. Elsevier, 2019, pp. 527–543.

[21] X. Zhao, "Introduction to bioactive materials in medicine," in *Bioactive Materials in Medicine: Design and Applications*, X. Zhao, J.M. Courtney, and H. Qian, Eds. Elsevier Inc., 2011, pp. 1–13.

[22] M. G. Yeo and G. H. Kim, "Fabrication of cell-laden electrospun hybrid scaffolds of alginate-based bioink and PCL microstructures for tissue regeneration," *Chem. Eng. J.*, vol. 275, pp. 27–35, 2015.

[23] H. Ahn *et al.*, "Engineered small diameter vascular grafts by combining cell sheet engineering and electrospinning technology," *Acta Biomater.*, vol. 16, no. 1, pp. 14–22, 2015.

[24] R. Dorati *et al.*, "Electrospun tubular vascular grafts to replace damaged peripheral arteries: A preliminary formulation study," *Int. J. Pharm.*, vol. 596, p. 120198, Feb. 2021.

[25] D. Hao *et al.*, "Rapid endothelialization of small diameter vascular grafts by a bioactive integrin-binding ligand specifically targeting endothelial progenitor cells and endothelial cells," *Acta Biomater.*, vol. 108, pp. 178–193, 2020.

[26] M. A. Nazeer, E. Yilgor, and I. Yilgor, "Electrospun polycaprolactone/silk fibroin nanofibrous bioactive scaffolds for tissue engineering applications," *Polymer (Guildf).*, vol. 168, pp. 86–94, 2019.

[27] J. Dulnik, D. Kołbuk, P. Denis, and P. Sajkiewicz, "The effect of a solvent on cellular response to PCL/gelatin and PCL/collagen electrospun nanofibres," *Eur. Polym. J.*, vol. 104, pp. 147–156, Jul. 2018.

[28] X. Zhou *et al.*, "Ca ions chelation, collagen I incorporation and 3D bionic

PLGA/PCL electrospun architecture to enhance osteogenic differentiation," *Mater. Des.*, vol. 198, p. 109300, Jan. 2021.
[29] O. Pereao *et al.*, "Chitosan/PEO nanofibers electrospun on metallized track-etched membranes: fabrication and characterization," *Mater. Today Chem.*, vol. 20, p. 100416, Jun. 2021.
[30] M. Zarei, A. Samimi, M. Khorram, M. M. Abdi, and S. I. Golestaneh, "Fabrication and characterization of conductive polypyrrole/chitosan/collagen electrospun nanofiber scaffold for tissue engineering application," *Int. J. Biol. Macromol.*, vol. 168, pp. 175–186, Jan. 2021.
[31] J. G. Fernandes *et al.*, "PHB-PEO electrospun fiber membranes containing chlorhexidine for drug delivery applications," *Polym. Test.*, vol. 34, pp. 64–71, Apr. 2014.
[32] C. Stani, L. Vaccari, E. Mitri, and G. Birarda, "FTIR investigation of the secondary structure of type I collagen: New insight into the amide III band," *Spectrochim. Acta Part A Mol. Biomol. Spectrosc.*, vol. 229, p. 118006, Mar. 2020.
[33] Y. Zhang, Z. Chen, X. Liu, J. Shi, H. Chen, and Y. Gong, "SEM, FTIR and DSC Investigation of Collagen Hydrolysate Treated Degraded Leather," *J. Cult. Herit.*, vol. 48, pp. 205–210, Mar. 2021.
[34] J. Spěváček, R. Konefał, J. Dybal, E. Čadová, and J. Kovářová, "Thermoresponsive behavior of block copolymers of PEO and PNIPAm with different architecture in aqueous solutions: A study by NMR, FTIR,
[35] V. M. Sonje et al., "Atorvastatin Calcium," Profiles Drug Subst. Excipients Relat. Methodol., vol. 35, pp. 1–70, Jan. 2010.
[36] P. Mounka, Y. Padavathi, A. Anjali, and N. P. REDDY, "Quantitative estimation of Atorvastatin calcium in bulk and tablet dosage forms using FTIR spectroscopy," Int. J. Pharma Bio Sci., vol. 9, no. 2, May 2018.